Ground-state cooling of multiple near-degenerate mechanical modes

Jin-Yu Liu,[1] Wenjing Liu,[1] Da Xu,[1] Jia-Chen Shi,[1] Haitan Xu,[2] Qihuang Gong,[1,3] and Yun-Feng Xiao[1,3,*]

[1]*State Key Laboratory for Mesoscopic Physics and Frontiers Science Center for Nano-optoelectronics, School of Physics, Peking University, Beijing 100871, China*

[2]*Shenzhen Institute for Quantum Science and Engineering, Southern University of Science and Technology, Shenzhen 518055, China*

[3]*Collaborative Innovation Center of Extreme Optics, Shanxi University, Taiyuan 030006, China*

(Received 31 August 2021; accepted 9 May 2022; published 23 May 2022)

We propose a general and experimentally feasible approach to realize simultaneous ground-state cooling of an arbitrary number of near-degenerate or even fully degenerate mechanical modes, overcoming the limit imposed by the formation of mechanical dark modes. Multiple optical modes are employed to provide different dissipation channels that prevent complete destructive interference of the cooling pathway, and thus eliminating the dark modes. The cooling rate and limit are explicitly specified, in which the distinguishability of the optical modes from the mechanical modes is found to be critical for an efficient cooling process. In a realistic multimode optomechanical system, ground-state cooling of all mechanical modes is demonstrated by sequentially introducing optical drives, proving the feasibility and scalability of the proposed scheme. The work may provide new insights in preparing and manipulating multiple quantum states in macroscopic systems.

DOI: 10.1103/PhysRevA.105.053518

I. INTRODUCTION

Optomechanics [1], exploring interactions between electromagnetic fields and mechanical vibrations, serves as an invaluable platform for studying macroscopic quantum phenomena such as macroscopic quantum coherence [2–8] and classical-to-quantum transition [9–11]. Application-wise, optomechanical sensors have demonstrated ultrahigh sensitivity in single-particle sensing and precision measurements of displacements, forces, and accelerations [12–14]. A premise of most of these applications is the ground-state cooling of the participating mechanical modes to suppress the thermal noise. However, thus far, though ground-state cooling has been investigated both theoretically [15–19] and experimentally [20–27] in a single mechanical mode, simultaneous cooling of multiple mechanical modes has not been demonstrated yet. This seriously limits the applications of multimode optomechanical systems in quantum many-body simulation [28–30], quantum information processing [31–34], and multiplexed sensing devices [35–39].

The major obstacle for multimode ground-state cooling is the formation of mechanical dark modes [40,41]. As the mode density of states increases with the size of the system, macroscopic resonators inevitably encounter multiple mechanical modes that are indistinguishable from the optical mode, i.e., their frequency differences become smaller than the optical linewidths. During the cooling processes, these modes hybridize and form dark modes that are decoupled from the optical field due to destructive interference [42,43], which prevents further cooling of the system. So far, several methods have been theoretically proposed to break the dark modes, either lifting the degeneracy of the mechanical modes [44,45] or inducing nonreciprocal energy flow [46–49]. However, their realizations need either additional coupling structures [44–48] or sophisticated control over the frequency and phase of multiple optical pumps [49] that are experimentally challenging. Moreover, the complexity increases drastically with increasing number of mechanical modes as interaction engineering is required between each pair of the mechanical modes. In this paper, we propose an alternative approach that is capable of simultaneous ground-state cooling of an arbitrary number of mechanical modes. Multiple optical modes effectively serve as different dissipation channels for phonons to break the destructive interference condition, and thereby prevent the formation of mechanical dark modes.

II. MODEL AND SOLUTION

A. Model of multimode optomechanical system

As shown in Fig. 1(a), we consider that multiple mechanical modes with frequencies ω_j and linewidths γ_j are coupled to multiple optical modes with frequencies ν_k and linewidths κ_k. The optical modes are chosen to be well separated to prevent cross-mode interactions. In the strong drive regime and in the rotation frame of the drive lasers, the linearized Hamiltonian of N mechanical modes and M optical modes reads (see Appendix A)

$$H = \vec{a}^\dagger \mathbf{\Delta} \vec{a} + \vec{b}^\dagger \mathbf{\Omega} \vec{b} + (\vec{a}^\dagger \boldsymbol{G} \vec{b} + \vec{a}^T \boldsymbol{G}^* \vec{b} + \text{H.c.}), \quad (1)$$

where $\vec{a} = (a_1, a_2, \ldots, a_M)^T$ is the vector of linearized annihilation operators of the cavity modes, and $\vec{b} = (b_1, b_2, \ldots, b_N)^T$ is the vector of linearized annihilation operators of the mechanical modes. The diagonal matrix $\mathbf{\Omega}$ describes the frequencies of the N mechanical modes, and

*yfxiao@pku.edu.cn

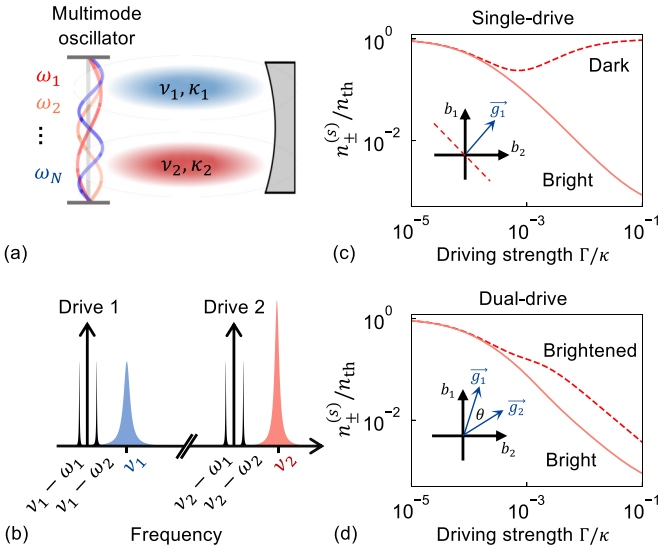

FIG. 1. (a) Schematic of a mechanical resonator supporting multiple mechanical modes coupled to an optical cavity. (b) The optical drive configuration of cooling two mechanical modes via two optical modes. (c)–(d) The normalized steady-state phonon number $n_\pm^{(s)}/n_{\rm th}$ depending on Γ/κ with single and dual drive, respectively. Here and hereafter, $\delta\omega_{\rm mec} = 0.001\kappa$, $\bar{\omega}_{\rm mec} = 20\kappa$.

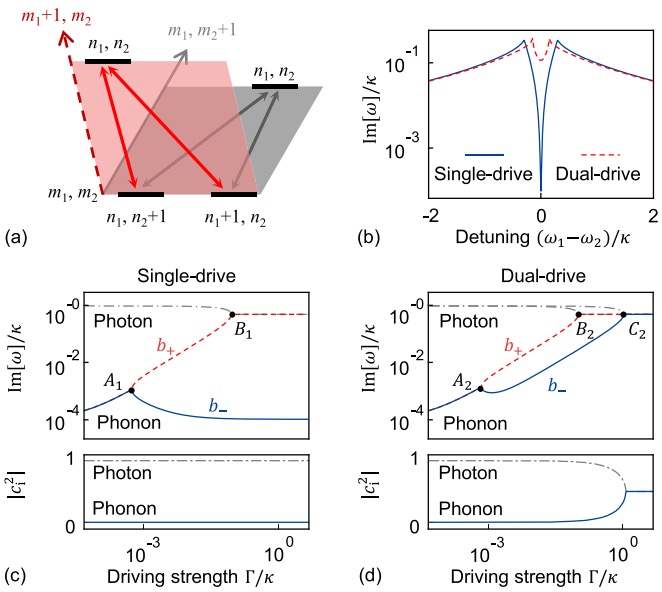

FIG. 2. (a) Schematic of the energy transfer pathways of two mechanical modes coupled with two optical drives. (b) Dissipation spectra of the mechanical modes under the single- (solid blue line) and dual-drive (dashed red line) conditions, both with $\Gamma = 0.1\kappa$. (c)–(d) The imaginary part of the eigenvalues Im[ω]/κ and the composition of the b_- mode, as a function of Γ/κ with single (c) and double (d) drive. The gray dash-dotted line, the dashed red line, and the solid blue lines denote the optical, b_+, and b_- modes. Here $\cos\theta = 0.8$.

the diagonal matrix $\mathbf{\Delta}$ denotes the detunings of the M drive lasers to their corresponding optical modes. $\boldsymbol{G}$ is the linearized coupling matrix, with element $g_{k,j}$ representing the coupling strength between the kth optical mode and jth mechanical mode. The optomechanical driving strength can be characterized by $\Gamma = \sum_{k=1}^{M} \Gamma_k$, with $\Gamma_k = \sum_{j=1}^{N} |g_{k,j}|^2/\kappa_k$ denoting the driving strength on the kth optical mode.

B. Analysis of bright and dark modes

We start the analysis with optomechanical cooling of two near-degenerate mechanical modes with frequencies ω_1 and ω_2, and linewidths γ_1 and γ_2, respectively. To optimize the optomechanical cooling, the drive lasers are set to the resolved red sideband of the corresponding optical modes with detuning $\delta_k = (\omega_1 + \omega_2)/2 = \bar{\omega}_{\rm mec}$ (see Appendix B), as presented in Fig. 1(b). To simplify the discussion, hereafter we assume $\kappa_1 = \kappa_2 = \kappa$, $\gamma_1 = \gamma_2 = \gamma = 10^{-4}\kappa$, and identical driving strength Γ_k of every optical mode. The discussion of general systems parameters can be found in Appendix B. By performing adiabatic approximation to Eq. (1), the optomechanical interaction can be effectively understood as a Γ-dependent coupling between the mechanical modes that gives rise to two new mechanical eigenmodes b_+ and b_-. As Γ exceeds the mechanical frequency difference $\delta\omega_{\rm mec} = |\omega_1 - \omega_2|$, $b_\pm$ become the hybridization of $b_{1,2}$. For a single optical drive, specifically, b_+ and b_- can be written as $(g_{k,1}b_1 + g_{k,2}b_2)/(g_{k,1}^2 + g_{k,2}^2)^{1/2}$ and $(-g_{k,2}b_1 + g_{k,1}b_2)/(g_{k,1}^2 + g_{k,2}^2)^{1/2}$ when $\Gamma \gg \delta\omega_{\rm mec}$. In the Hilbert space spanned by b_1 and b_2, eigenmode $b_\pm$ correspond to the vectors along and perpendicular to the optomechanical coupling vector $\vec{g}_k = (g_{k,1}, g_{k,2})$, respectively, as shown in the inset of Fig. 1(c). Hence, b_+ is strongly coupled to the optical field and termed the *bright* mode, while b_- is completely decoupled and termed the *dark* mode.

Figure 1(c) plots the steady-state phonon number of each mechanical eigenmode, $n_\pm^{(s)} = \langle b_\pm^\dagger b_\pm \rangle$, normalized to the thermal phonon number $n_{\rm th} \approx (e^{\hbar\bar{\omega}_{\rm mec}/kT} - 1)^{-1}$. The Born-Markov approximation is applied in the calculation of steady-state phonon number here and hereafter, as no dominant mode exists in the thermal bath (see Appendix B). While both mechanical modes can be cooled at weak optical drives, from the onset of the mechanical strong coupling, the bright and dark modes start to behave distinctly. Although the bright mode is further cooled down, the dark mode is heated up due to its gradual decoupling from the optical modes [40,46]. Particularly, $n_-^{(s)}$ approaches $n_{\rm th}$ at $\Gamma \gg \delta\omega_{\rm mec}$, indicating the complete suppression of the optomechanical cooling. Such suppression acts as one of the major obstacles in the cooling of multimode mechanical oscillators, which has been widely observed in experiments [42,43]. We propose that this challenge can be resolved when a second optical mode is adopted for cooling, as seen in Fig. 1(d). Upon introduction of the second coupling vector $\vec{g}_{k'} = (g_{k',1}, g_{k',2})$, as long as the two coupling vectors $\vec{g}_k$ and $\vec{g}_{k'}$ are not collinear ($\theta \neq 0$), no mechanical mode can be decoupled from both optical modes. Indeed, in this case, both mechanical modes can be efficiently cooled either before or after the mechanical strong coupling.

From the energy transfer aspect, different optical modes serve as different dissipation channels for phonons in optomechanical cooling. With a single optical drive, near-degenerate phonon modes decaying through the same channel interfere destructively with each other, analogous to the electromagnetic induced transparency (EIT), as shown in Fig. 2(a) [50].

Within the transparency window, the mechanical mode is decoupled from the optical field with its damping rate reduced to the intrinsic linewidth γ [Fig. 2(b). When multiple optical pathways are present, phonon dissipation forbidden in one pathway can decay through another, which effectively removes the EIT window and brightens up the dark mode.

The evolution of the mechanical dark mode can be quantitatively investigated by the eigenvalues and eigenvectors of the system, as shown in Figs. 2(c) and 2(d). At $\Gamma \approx \delta\omega_{\rm mec}$, exceptional points are present at A_1 and A_2 in the single- and dual-drive schemes, respectively, indicating the formation of the bright and dark mechanical modes. In both cases, the bright modes b_+ (red curves) exhibit rapid dissipation rate increases, quickly reaching their classical cooling limits at the second exceptional points of the strong optomechanical coupling, denoted by B_1 and B_2, respectively. On the other hand, right after the exceptional points A_1 and A_2, the dissipation rates of both b_- modes (blue curves) decrease as the driving strengths grow. In the single-drive scheme, it decreases monotonically to the intrinsic dissipation of the mechanical mode γ, hence the cooling is completely suppressed. Oppositely, in the proposed dual-drive scheme, the b_- mode is brightened up and eventually reaches an emerging exceptional point C_2. Meanwhile, the eigenvectors show that in the single-drive scheme the mechanical dark mode becomes purely phononic with strong optical drive, while in the dual-drive scheme it is significantly hybridized with the photonic modes. The brightened b_- mode exhibits its classical cooling limit when reaching point C_2, which is characterized by $n_-^{(s)} = \gamma n_{\rm th}/(\gamma+\kappa)$. This value recovers the cooling limit of the single-mechanical-mode system, demonstrating the elimination of the dark mode effect. It should also be noted that the quantum cooling limit of the multimode system can be estimated as $\kappa^2/(16\bar{\omega}_{\rm mec}^2)$, and, at the condition under investigation, it is 2 orders of magnitude smaller than the classical limit. The details of the calculation are presented in Appendix C.

C. Solution of steady-state phonon number

While the restriction on the cooling limit can be lifted by any drive configuration with noncollinear coupling vectors, a further optimization of the system parameters that can minimize the required driving strength is important for experimental realizations. Quantitatively, the steady-state total phonon number $n_{\rm tot}^{(s)} = n_+^{(s)} + n_-^{(s)}$ at a given driving strength Γ is calculated in Appendix B, in the drive range where the bright and dark modes are formed but the system still remains in the weak coupling regime:

$$n_{\rm tot}^{(s)} = \frac{2\gamma n_{\rm th}(\gamma+2\Gamma)}{\gamma^2+4\gamma\Gamma+4\Gamma^2\sin^2\theta}. \tag{2}$$

It can be seen that the angle θ is the key parameter for achieving efficient cooling, which describes the distinguishability of the optical modes to the mechanical modes. At $\Gamma \gg \gamma$, when $\theta = 0$, $n_{\rm tot}^{(s)} \approx n_{\rm th}$, the system is equivalent to being driven by a single optical pump, and the cooling is suppressed. When $\theta \neq 0$, $n_{\rm tot}^{(s)} \approx n_{\rm th}\gamma/(\Gamma\sin^2\theta)$, indicating that the cooling is more efficient when the chosen optical modes exhibit more distinct coupling strengths from the mechanical modes. Especially, when $\theta = \pi/2$, $n_{\rm tot}$ reaches the minimum at a given Γ. In this case, each drive interacts exclusively with the b_+ or b_- mode, and the system can be reduced to a single-mechanical-mode resonator.

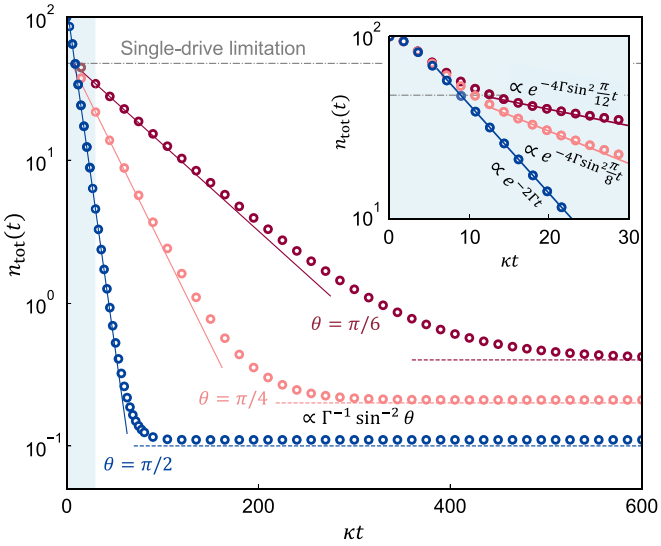

FIG. 3. Temporal evolution of the total phonon number $n_{\rm tot}(t)$ during the cooling process. Hollow circles denote the numerically calculated phonon number; solid and dashed lines represent the analytically calculated phonon decay rate and the steady-state phonon number, respectively; the dash-dotted line denotes the steady-state phonon number cooled by a single-optical drive. Inset: the zoomed-in plot of $\kappa t = [0, 30]$, represented by the blue shaded region in the main figure. Here $\Gamma = 0.05\kappa$ and $n_{\rm tot}(0) = 100$.

D. Time domain evolution of cooling process

The cooling speed is another important figure of merit for optomechanical cooling processes. Here, the temporal evolution of the total phonon number $n_{\rm tot}(t)$ is calculated numerically with the fourth-order Runge-Kutta method, as shown in Fig. 3. The optical drives are turned on at $\kappa t = 0$ and kept constant at $\Gamma = 0.05\kappa$. For $0 < \theta < \pi/2$, $n_{\rm tot}(t)$ is characterized by a double-exponential decay, with the fast and slow processes, $\exp[-4\Gamma\cos^2(\theta/2)t]$ and $\exp[-4\Gamma\sin^2(\theta/2)t]$ corresponding to the b_+ and b_- modes, respectively. At small κt, the system exhibits a rapid phonon dissipation of both mechanical modes, characterized by a θ-independent decay rate of Γ, till the cooling limitation of the single-drive configuration (gray dotted line), as shown in the inset of Fig. 3. Below the single-drive limitation line, most phonons in the b_+ mode have already been dissipated from the system due to the larger decay rate, and thus the process is dominated by the b_- mode. In this regime, a large θ results in a significantly accelerated phonon decay rate. In particular, for the case $\theta = \pi/2$, the system reduces to the single-mechanical-mode cooling case with a monoexponential decay rate of Γ, until reaching the steady state. Meanwhile, the steady-state phonon number $n_{\rm tot}$ also decreases while increasing θ, and the numerical results match well with the analytical solution described by Eq. (2).

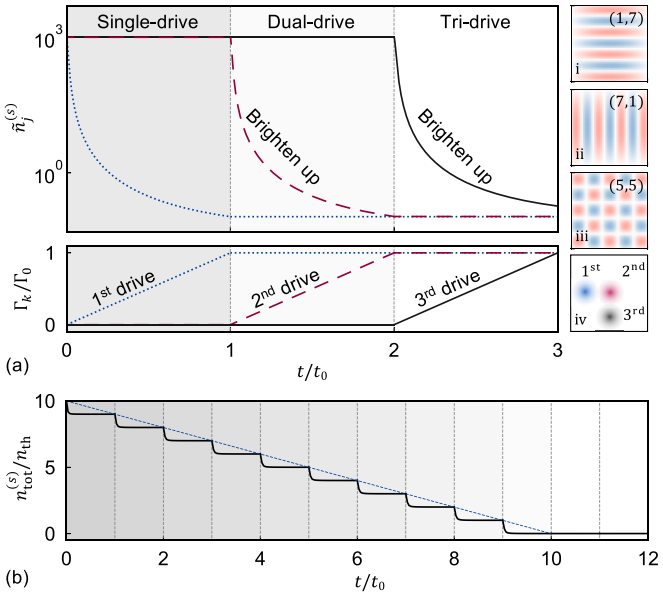

FIG. 4. (a) Evolution of the steady phonon number $\tilde{n}_j^{(s)}$ of each mechanical eigenmode (upper panel), as three optical drives are quasistatically introduced (lower panel). The mechanical modes are fully degenerate with $\omega_j/2\pi = 1.178\,\mathrm{MHz}$, $\gamma_j/2\pi = 39.0\,\mathrm{mHz}$, and their mode profiles are presented in i–iii; Optical modes have the linewidths of $\kappa_k/2\pi = 0.967\,\mathrm{MHz}$ and $\Gamma_0 = 980\,\mathrm{Hz}$. The spatial profiles are shown in iv. (b) Evolution of $n_{\mathrm{tot}}^{(s)}$ of a $N = 10$ system as 12 optical drives are introduced sequentially. In each regime divided by the vertical dashed lines, one optical drive is turned on and increased from 0 to $\Gamma_0 = 0.1\kappa$, and t_0 is an arbitrary timescale which satisfies $t_0 \gg \gamma_j^{-1}$, to make sure that the system is in the quasistatic limit throughout the evolution.

III. GENERALIZATION TO *N*-MECHANICAL-MODE SYSTEM

Finally, we present here that our method can be straightforwardly generalized to arbitrary number of mechanical modes. In the N dimensional Hilbert space of mechanical modes, a mode is dark if it is orthogonal to all the coupling vectors $\vec{g}_k = (g_{k,1}, g_{k,2}, \ldots, g_{k,N})$. Hence, a dark subspace can be defined as the orthogonal complement of the span of all coupling vectors. When M optical modes with linearly independent coupling vectors are introduced, the dimension of dark subspace is reduced to $N - M$. Given that $M \geqslant N$, all dark modes are eliminated and the ground-state cooling for N degenerate mechanical modes can be achieved.

As an example, a silicon nitride membrane with clamped boundaries inserted into a Fabry-Pérot optical cavity is considered, with all the optomechanical parameters corresponding to realistic experimental systems [51–54]. Cooling of the threefold degenerate mechanical drum modes (1,7), (7,1), and (5,5) is demonstrated, with three spatially distinct optical modes employed to allow large θ, as shown in Fig. 4(a), i–iv. This drive scheme can be realized by focusing the laser drive onto different positions of the membrane and adjusting the membrane position in the cavity [51]. The three optical drives are turned on sequentially in the quasistatic limit to examine the phonon number evolution of the three mechanical modes. When the first drive is turned on and its strength Γ_1 is increased from 0 to Γ_0, the three mechanical modes hybridize to form one bright mode ($\tilde{b}_1$, blue curve) and two dark modes ($\tilde{b}_2$ and $\tilde{b}_3$, black and magenta curves, respectively). Once turning on the second drive, one of the dark modes $\tilde{b}_2$ is brightened up, leaving only one dark mode in the system. All three modes are effectively turned bright and cooled down to $\tilde{n}_j^{(s)} < 1$ when the third drive is on, achieving simultaneous ground-state cooling of all three mechanical modes under investigation. We note that the cooling is independent of the drive sequence as the system is linearized with a unique steady state, e.g., the steady state phonon number remains the same when all three drives are induced at the same time.

For a more general demonstration, the analysis is further pushed to the cooling process of more mechanical modes, for example $N = 10$. With 12 drives quasi-statically introduced and linearly enhanced in sequence, the result is shown in Fig. 4(b). When $M < 10$, in the presence of a new optical drive, $n_{\mathrm{tot}}^{(s)}$ undergoes a significant decrease and reaches a cooling limit at $n_{\mathrm{tot}}^{(s)} \approx (10 - M)n_{\mathrm{th}}$, neglecting the phonon occupancy of the bright modes, as represented by the blue dashed line. This steplike cooling curve indicates the successive elimination of the dark modes by each optical drive, as predicted by the theory. When $M \geqslant 10$, all dark modes have been eliminated, and further introduction of additional optical modes no longer leads to significant cooling other than the increase of the total drive strength.

As for the cooling limit, when M drives with $M = N$ are employed and all the dark modes are eliminated, $n_{\mathrm{tot}}^{(s)}$ in weak coupling regime can be asymptotically described by (see Appendix B)

$$n_{\mathrm{tot}}^{(s)} = \tfrac{1}{4}\gamma\kappa n_{\mathrm{th}}\, \|\boldsymbol{G}^{-1}\|_2, \tag{3}$$

where $\|\boldsymbol{G}^{-1}\|_2 = \sum_{k,j=1}^{N} |(g^{-1})_{k,j}|^2$. Here, $\boldsymbol{G}^{-1}$ exists if and only if all the coupling vectors are linearly independent. For each $\vec{g}_k$, the rest coupling vectors span an $N - 1$ dimensional hypersurface in the N dimensional Hilbert space. For linearly independent coupling vectors, the cross angle θ_k between $\vec{g}_k$ and this hypersurface is nonzero, and the cooling limit can be rewritten as (see Appendix B)

$$n_{\mathrm{tot}}^{(s)} = \frac{\gamma n_{\mathrm{th}}}{4} \sum_{k=1}^{N} \frac{1}{\Gamma_k \sin^2\theta_k} \qquad (\theta_k \neq 0). \tag{4}$$

Hence a larger $\sin^2\theta_k$ can result in a better cooling performance. Also, if all Γ_k are kept constant, the best cooling is achieved when all $\theta_k = \pi/2$ for $k = 1, 2, \ldots, N$. In this case, each optical mode solely couples to one mechanical mode. This result provides a quantitative guidance for selecting the optical modes that are most suitable for cooling a multiple mechanical mode system.

IV. CONCLUSION

In this paper, we have proposed a general scheme to realize the ground-state cooling of near-degenerate or even degenerate mechanical modes. Different optical modes provide different dissipation channels that can effectively eliminate the mechanical dark modes that obstruct the cooling process. The distinguishability of the optical modes from the mechanical modes is found to be an essential factor that allows efficient optomechanical cooling. This approach not

only provides an experimentally feasible method that may help to solve one of the critical challenges in fundamental and applied studies on macroscopic optomechanics, but could also inspire dark mode manipulation and suppression in analogous systems such as cold atom ensembles.

ACKNOWLEDGMENTS

J.-Y.L., W.L., and D.X. contributed equally. This project is supported by the National Key R&D Program of China (Grant No. 2018YFA0704404) and the National Natural Science Foundation of China (Grants No. 11825402, No. 11654003, No. 61435001, No. 62175002, No. 92150301, No. 11974031, and No. 62035017).

APPENDIX A: DERIVATION OF THE LINEARIZED HAMILTONIAN OF A MULTIMODE OPTOMECHANICAL SYSTEM

The Hamiltonian of an optically driven multimode optomechanical system can be generally written as

$$H = H_{\text{free}} + H_{\text{int}} + H_{\text{drive}}. \tag{A1}$$

Here, H_{free} is the free Hamiltonian of the optical and mechanical modes with

$$H_{\text{free}} = \sum_{k=1}^{M} \hbar \nu_k a_k^\dagger a_k + \sum_{j=1}^{N} \hbar \omega_j b_j^\dagger b_j, \tag{A2}$$

where $a_k(a_k^\dagger)$ is the annihilation (creation) operator of the kth optical mode with frequency ν_k and linewidth κ_k; b_j $(b_j^\dagger)$ is the annihilation (creation) operator of the jth mechanical mode with frequency ω_j and linewidth γ_j. These operators obey the bosonic commutation relations

$$[a_k, a_{k'}^\dagger] = \delta_{kk'}, \quad [b_j, b_{j'}^\dagger] = \delta_{jj'}, \quad [a_k, b_j^{(\dagger)}] = 0. \tag{A3}$$

H_{int} represents the interaction Hamiltonian between the optical and mechanical modes [55],

$$H_{\text{int}} = \hbar \sum_{k=1}^{M} \sum_{j=1}^{N} g_{k,j}^S a_k^\dagger a_k (b_j^\dagger + b_j), \tag{A4}$$

where $g_{k,j}^S$ is the single photon coupling strength between the kth optical mode and the jth mechanical mode.

H_{drive} describes the laser drive on the optical modes,

$$H_{\text{drive}} = \sum_{k=1}^{M} Q_k e^{-i\omega_k^d t} a_k^\dagger + \text{H.c.}, \tag{A5}$$

where Q_k is the driving amplitude and ω_k^d is the driving frequency for the kth optical mode.

In the rotating frames of the drive lasers $S[t] = \exp[-it\sum \omega_k^d a_k^\dagger a_k]$, the optical operators are transformed to $S^\dagger[t] a_k S[t] = a_k e^{-i\omega_k^d t}$. The Hamiltonian is transformed to $H' = S^\dagger[t] H S[t] - i\hbar S^\dagger[t]\partial_t S[t]$ and written as

$$H'_{\text{free}} = \sum_{k=1}^{M} \hbar \delta'_k a_k^\dagger a_k + \sum_{j=1}^{N} \hbar \omega_j b_j^\dagger b_j, \tag{A6}$$

$$H'_{\text{int}} = H_{\text{int}}, \tag{A7}$$

$$H'_{\text{drive}} = \sum_{k=1}^{M} Q_k a_k^\dagger + \text{H.c.}, \tag{A8}$$

where the original drive detuning $\delta'_k = \nu_k - \omega_k^d$. With the Born-Markov approximation, the Langevin equations of the system can therefore be written as

$$\frac{da_k}{dt} = \left(-i\delta'_k - \frac{\kappa_k}{2}\right) a_k - i \sum_{j=1}^{N} g_{k,j}^S a_k (b_j^\dagger + b_j) - iQ_k - \sqrt{\kappa_k} a_k^{\text{in}}(t), \tag{A9}$$

$$\frac{db_j}{dt} = \left(-i\omega_j - \frac{\gamma_j}{2}\right) b_j - i \sum_{k=1}^{M} g_{k,j}^S a_k^\dagger a_k - \sqrt{\gamma_j} b_j^{\text{in}}(t), \tag{A10}$$

where $a_k^{\text{in}}, b_j^{\text{in}}$ are the input operators of the optical and mechanical modes, which obey

$$\left\langle {a_k^{\text{in}}}^\dagger(t_k) a_{k'}^{\text{in}}(t_{k'}) \right\rangle = \delta_{kk'} \delta(t_k - t_{k'}) n_{\text{th}}(\nu_k), \tag{A11}$$

$$\left\langle {b_j^{\text{in}}}^\dagger(t_j) b_{j'}^{\text{in}}(t_{j'}) \right\rangle = \delta_{jj'} \delta(t_j - t_{j'}) n_{\text{th}}(\omega_j). \tag{A12}$$

Here the thermal noise $n_{\text{th}}(\omega) = 1/(e^{\hbar\omega/kT} - 1)$ with T being the environment temperature. The thermal bath is composed of numerous free-space electromagnetic modes, which all couple weakly to the system. As no dominant mode exists in the thermal bath, the back action on the thermal bath can be ignored and the Markov approximation is applicable. As the high optical frequency condition $\hbar\nu_k \gg kT$ applies for common experimental conditions, thermal noise $n_{\text{th}}(\nu_k) \approx 0$ for the optical modes. The mechanical modes are nearly degenerate with $\omega_j \approx \bar{\omega}_{\text{mec}} = (\sum_{j=1}^{N} \omega_j)/N$, thus all $n_{\text{th}}(\omega_j) \approx n_{\text{th}}(\bar{\omega}_{\text{mec}})$, labeled as n_{th} hereafter. The remaining independent quadratic expressions of $a_k^{\text{in}(\dagger)}$, $b_j^{\text{in}(\dagger)}$ have zero value expectations.

The operators $o \in \{a_k^{(\dagger)}, b_j^{(\dagger)}\}$ can be divided into their expectations and fluctuations, $o = \langle o \rangle + \delta o$. Defining $\alpha_k = \langle a_k \rangle$ and $\beta_j = \langle b_j \rangle$, the Langevin equations are split into equations of the expectations,

$$\frac{d\alpha_k}{dt} = \left(-i\delta'_k - \frac{\kappa_k}{2}\right) \alpha_k - i \sum_{j=1}^{N} g_{k,j}^S \alpha_k (\beta_j^* + \beta_j) - iQ_k, \tag{A13}$$

$$\frac{d\beta_j}{dt} = \left(-i\omega_j - \frac{\gamma_j}{2}\right) \beta_j - i \sum_{k=1}^{M} g_{k,j}^S \alpha_k^* \alpha_k, \tag{A14}$$

and equations of the fluctuations,

$$\frac{d\delta a_k}{dt} = \left(-i\delta_k - \frac{\kappa_k}{2}\right) \delta a_k - \sqrt{\kappa_j} a_j^{\text{in}}(t) - i \sum_{j=1}^{N} g_{k,j} (\delta b_j^\dagger + \delta b_j), \tag{A15}$$

$$\frac{d\delta b_j}{dt} = \left(-i\omega_j - \frac{\gamma_j}{2}\right) \delta b_j - \sqrt{\gamma_j} b_j^{\text{in}}(t) - i \sum_{k=1}^{M} (g_{k,j} \delta a_k^\dagger + g_{k,j}^* \delta a_k), \tag{A16}$$

where the corrected drive detuning and the linear coupling strength are defined as $\delta_k = \delta'_k + \sum_{j=1}^{N} g_{k,j}(\beta_j^* + \beta_j)$ and $g_{k,j} = g_{k,j}^S \alpha_k$, respectively, for the kth optical mode and the jth mechanical mode. The steady-state expectations of the optical and mechanical modes at $d\langle o^{(\dagger)}\rangle/dt = 0$ are

$$\alpha_k = \frac{-iQ_k}{i\delta_k + \kappa_k/2}, \tag{A17}$$

$$\beta_j = \frac{i\sum_{k=1}^{M} g_{k,j}^S |\alpha_k|^2}{i\omega_j + \gamma_j/2}. \tag{A18}$$

The above Langevin equations of fluctuations are equivalent to the linearized Hamiltonian

$$H_L = \sum_{j=1}^{N} \omega_j \delta b_j^\dagger \delta b_j + \sum_{k=1}^{M} \delta_k \delta a_k^\dagger \delta a_k + \sum_{j=1}^{N}\sum_{k=1}^{M} [g_{k,j}\delta a_k^\dagger (\delta b_j + \delta b_j^\dagger) + \text{H.c.}]. \tag{A19}$$

In the main text and in the following appendices, all the symbols $(\delta a, \delta b)$ are relabeled as (a, b) for simplicity.

APPENDIX B: CALCULATION OF THE STEADY-STATE PHONON NUMBER

The steady-state phonon number is calculated via the Lyapunov equation derived from the quantum master equation [56], and the steady-state phonon number of a mechanical mode $\tilde{b}_j = \sum_{j'=1}^{N} e_{jj'} b_{j'}$ is written as

$$\tilde{n}_j^{(s)} = \langle \tilde{b}_j^\dagger \tilde{b}_j \rangle = \sum_{j'=1}^{N}\sum_{j''=1}^{N} e_{jj'}^* e_{jj'} \langle b_{j'}^\dagger b_{j''} \rangle \tag{B1}$$

Analytically, further applying the rotating wave approximation at the red sideband ($\delta_k = \bar{\omega}_{\text{mec}}$) and the adiabatic approximation in the weak coupling regime ($g_{k,j} \ll \kappa_{k'}$), terms $\langle oo' \rangle^{(*)}$ can be ignored, and the Fourier transformed Langevin equations of a_k are

$$a_k(\omega) = \frac{-i\sum_{j=1}^{N} g_{k,j} b_j(\omega) - \sqrt{\kappa}_k a_k^{\text{in}}(\omega)}{i\delta_k - i\omega + \frac{\kappa_k}{2}}. \tag{B2}$$

When returning to the time domain, the difference between $b_j(\omega)$ and $b_j(\omega_j)\delta(\omega - \omega_j)$ can be ignored for $g_{k,j} \ll \kappa_{k'}$, thus a_k is expressed as

$$a_k = \sum_{j=1}^{N} \frac{-ig_{k,j} b_j}{i\delta_k - i\omega_{j'} + \frac{\kappa_k}{2}}. \tag{B3}$$

Assuming that the mechanical modes are optically indistinguishable ($|\omega_j - \omega_{j'}| \ll \kappa_k$), and that all the drives are located at the red sideband with $\delta_k = \bar{\omega}_{\text{mec}} \approx \omega_j$, Eq. (B3) can be simplified as

$$a_k = \sum_{j=1}^{N} \frac{-2ig_{k,j} b_j}{\kappa_k}. \tag{B4}$$

After substituting Eq. (B4) into Eq. (A16), the latter becomes

$$\frac{db_j}{dt} = \left(-i\omega_j - \frac{\gamma_j}{2}\right) b_j - 2\sum_{j'=1}^{N}\sum_{k=1}^{M} \frac{g_{k,j}^* g_{k,j'} b_{j'}}{\kappa_k} - \sqrt{\gamma_j} b_j^{\text{in}}(t). \tag{B5}$$

The second term on the right-hand side of Eq. (B5) represents the optically induced damping, of which the Hermitian operator is defined in the matrix form as

$$\boldsymbol{P} = 2\boldsymbol{G}^\dagger \boldsymbol{K}^{-1} \boldsymbol{G}. \tag{B6}$$

where $k_{kk'} = \kappa_k \delta_{kk'}$. This operator $\boldsymbol{P}$ represents the dissipation of the mechanical modes induced by the all the optical modes, which can be decomposed as

$$\boldsymbol{P} = \sum_{k=1}^{M} \boldsymbol{P}^{(k)}, \tag{B7}$$

$$p_{jj'}^{(k)} = 2\frac{g_{k,j}^* g_{k,j'}}{\kappa_k}. \tag{B8}$$

Operator $\boldsymbol{P}$ can be viewed as the dissipation induced by the kth optical mode which only depends on the driving strength Γ_k. Each $\boldsymbol{P}^{(k)}$ is proportional to the projection operator along $\vec{g}_k^* = (g_{k,1}^*, g_{k,2}^*, \ldots, g_{k,N}^*)$. As a result, $\boldsymbol{P}^{(k)}$ cannot cool down any $\tilde{b}_j$ with coefficient vector $\vec{e}_j = (e_{j,1}, e_{j,2}, \ldots, e_{j,N})^T$ orthogonal to $\vec{g}_k$.

By substituting Eq. (B6) into Eq. (A16), the Langevin equations of b_j is rewritten as

$$\frac{db_j}{dt} = \left(-i\omega_j - \frac{\gamma_j}{2}\right) b_j - \sum_{j'=1}^{N} p_{jj'} b_{j'} - \sqrt{\gamma_j} b_j^{\text{in}}(t). \tag{B9}$$

The corresponding effective mechanical Hamiltonian can thus be defined as

$$H_{\text{eff}} = H_0 - iD = \sum_{j=1}^{N} \hbar\omega_j b_j^\dagger b_j - i\sum_{j=1}^{N}\sum_{j'=1}^{N} b_j^\dagger p_{jj'} b_{j'}, \tag{B10}$$

with the master equation [56] given by

$$\frac{d\rho}{dt} = \frac{i}{\hbar}[\rho, H_0] - \frac{1}{\hbar}[D, \rho]_+ + \frac{2}{\hbar}\rho\,\text{Tr}[\rho D] + \sum_{j=1}^{N} \frac{\gamma_j(n_{\text{th}}+1)}{2}[2b_j\rho b_j^\dagger - b_j^\dagger b_j \rho - \rho b_j^\dagger b_j] + \sum_{j=1}^{N} \frac{\gamma_j n_{\text{th}}}{2}[2b_j^\dagger \rho b_j - b_j b_j^\dagger \rho - \rho b_j b_j^\dagger]. \tag{B11}$$

Here, the steady state phonon can be calculated as $\langle b_j^\dagger b_{j'} \rangle = \text{Tr}[\rho b_j^\dagger b_{j'}]$. The nonlinear terms $\langle b_j^\dagger b_{j'}^\dagger b_{j''} b_{j'''} \rangle$ and $\langle b_j^\dagger b_{j'} \rangle \langle b_{j''}^\dagger b_{j'''} \rangle$ are expected to be very small ($\langle b_j^\dagger b_{j'} \rangle \ll n_{\text{th}}$)

and can be ignored, which simplifies the Lyapunov equation to

$$\frac{d}{dt}\langle b_{j'}^{\dagger} b_j\rangle = \left(i\omega_{j'} - i\omega_j - \frac{\gamma_j+\gamma_{j'}}{2}\right)\langle b_{j'}^{\dagger} b_j\rangle - \sum_{j''=1}^{N}[p_{jj''}\langle b_{j'}^{\dagger} b_{j''}\rangle + p_{j'j''}\langle b_{j''}^{\dagger} b_j\rangle] + \gamma_j \delta_{j'j} n_{\rm th}. \tag{B12}$$

In the case of $M = N = 2$ and with symmetric parameters $\kappa_1 = \kappa_2 = \kappa$, $\gamma_1 = \gamma_2 = \gamma$, and $\Gamma_1 = \Gamma_2 = \Gamma$ assumed, the steady-state total phonon number reads

$$n_{\rm tot}^{(s)} = \frac{2\gamma n_{\rm th}(\gamma+2\Gamma)}{(\gamma+2\Gamma)^2 - 4\Gamma^2\cos^2\theta\,\frac{(\gamma+2\Gamma)^2}{(\gamma+2\Gamma)^2+\delta\omega_{\rm mec}^2}}, \tag{B13}$$

in which $\delta\omega_{\rm mec} = |\omega_1 - \omega_2|$, and θ denotes the cross angle between the coupling vectors $\vec{g}_1$ and $\vec{g}_2$ with $0 \leqslant \theta \leqslant \pi/2$.

With $\delta\omega_{\rm mec} \ll \Gamma$, Eq. (B13) is simplified to Eq. (2) of the main text.

The analysis is then extended to systems with $N > 2$, in which the coupling vectors are chosen to be linearly independent. When the number of optical modes $M < N$, dark modes exist. As the phonon numbers of the dark modes are approximately $n_{\rm th}$ and far outweigh those of the bright modes, the total phonon number $n_{\rm tot}^{(s)} \approx (N-M)n_{\rm th}$.

When $M \geqslant N$, all dark modes are eliminated and the above approximation fails. As M exceeds N, the new optical modes inevitably have linearly dependent coupling vectors with the existing N optical modes, which can be simply recognized as a increase of their drive strengths. Therefore, the following calculations focus on the $M = N$ case. By assuming $\gamma_j = \gamma$, and γ, $\delta\omega_{\rm mec} \ll \Gamma_k$, the Lyapunov equation becomes

$$\boldsymbol{P}^T\boldsymbol{V} + \boldsymbol{V}\boldsymbol{P}^T = \gamma n_{\rm th}\boldsymbol{I}, \tag{B14}$$

where $v_{j'j} = \langle b_{j'}^{\dagger} b_j\rangle$ and $n_{\rm tot}^{(s)} = {\rm Tr}\,\boldsymbol{V}$. As $\boldsymbol{P}$ is Hermitian, it is unitarily diagonalizable as $\boldsymbol{P}^T = \boldsymbol{S}^{\dagger}\boldsymbol{\Lambda}\boldsymbol{S}$, with diagonal elements $\lambda_{j'j} = \lambda_j\delta_{j'j}$ and the unitary matrix $\boldsymbol{S}$ satisfying $\boldsymbol{S}^{\dagger}\boldsymbol{S} = \boldsymbol{I}$. After the substitution, Eq. (B14) can be rewritten as

$$[\boldsymbol{S}\boldsymbol{V}\boldsymbol{S}^{\dagger}]_{j'j} = \frac{\gamma n_{\rm th}\delta_{j'j}}{2\lambda_j}, \tag{B15}$$

$$n_{\rm tot}^{(s)} = {\rm Tr}\,\boldsymbol{V} = \frac{\gamma n_{\rm th}}{2}\sum_{j=1}^{N}\lambda_j^{-1} = \frac{\gamma n_{\rm th}}{2}{\rm Tr}[\boldsymbol{P}^{-1}]. \tag{B16}$$

Substituting Eq. (B6),

$${\rm Tr}[\boldsymbol{P}^{-1}] = \frac{\kappa}{2}\,\|\boldsymbol{G}^{-1}\|_2, \tag{B17}$$

$$n_{\rm tot}^{(s)} = \frac{\kappa}{4}\gamma\kappa n_{\rm th}\,\|\boldsymbol{G}^{-1}\|_2\,. \tag{B18}$$

The parameter θ_k is defined as the cross angle between $\vec{g}_k$ and the hypersurface spanned by the rest of the coupling vectors, which can be expressed as

$$\theta_k = \arcsin\frac{\vec{g}_k^{*}\cdot\vec{c}_k}{|\vec{g}_k||\vec{c}_k|}, \tag{B19}$$

where $\vec{c}_k$ is reciprocal vector of $\vec{g}_k$, satisfying $\vec{g}_k^{*}\cdot\vec{c}_j = \delta_{kj}$ and $0 \leqslant \theta_k \leqslant \pi/2$. Vectors $\vec{c}_k$ can be organized into a matrix $\boldsymbol{C} = (\boldsymbol{G}^{\dagger})^{-1}$, and by substituting $\boldsymbol{C}$ into Eq. (B16) it is derived that

$$n_{\rm tot}^{(s)} = \frac{\gamma n_{\rm th}}{4}{\rm Tr}\,\boldsymbol{G}^{-1}\boldsymbol{K}\boldsymbol{G}^{\dagger-1} = \frac{\gamma n_{\rm th}}{4}{\rm Tr}\boldsymbol{C}^{\dagger}\boldsymbol{K}\boldsymbol{C} = \frac{\gamma n_{\rm th}}{4}\sum_{k=1}^{N}\kappa_k|\vec{c}_k|^2 = \frac{\gamma n_{\rm th}}{4}\sum_{k=1}^{N}\frac{1}{\Gamma_k\sin^2\theta_k}, \tag{B20}$$

where $\Gamma_k = |\vec{g}_k|^2/\kappa_k$.

APPENDIX C: CALCULATION OF THE CLASSICAL AND QUANTUM PARTS OF THE COOLING LIMIT

The classical cooling limit is reached when the system enters the optomechanical strong coupling regime. In this regime, the adiabatic elimination of the optical modes, Eq. (B3), no longer applies. In the sideband-resolved regime, the classical cooling limit is obtained by solving Lyapunov equations.

When $M = N = 2$, the steady-state total phonon number of the two mechanical modes can be solved as

$$n_{\rm tot}^{(s)} = \frac{2Ln_{\rm th}}{L + 2s + 4\sin^2\theta - \frac{4s^2\cos^2\theta}{L+2s+4\sin^2\theta}}, \tag{C1}$$

where $L = \gamma[(s+2)^2 - 4\cos^2\theta]/\kappa$ and $s = (\gamma+\kappa)/\Gamma$. Here, symmetric parameters $\delta\omega_{\rm mec} = 0$, $\gamma_1 = \gamma_2 = \gamma$, $\kappa_1 = \kappa_2 = \kappa$, $\Gamma_1 = \Gamma_2 = \Gamma/2$ are assumed.

For any $\theta \neq 0$ and $s \approx 0$,

$$n_{\rm tot}^{(s)} = \frac{2\gamma n_{\rm th}}{\gamma+\kappa}. \tag{C2}$$

If $\theta = 0$, the same condition leads to

$$n_{\rm tot}^{(s)} = \left(\frac{\gamma}{\gamma+\kappa} + 1\right)n_{\rm th}. \tag{C3}$$

The quantum cooling limit is calculated by the force noise power spectral density $S_j^{FF}(\omega) = \int_{-\infty}^{\infty}\langle F_j(t)F_j(0)\rangle e^{i\omega t}$. The optical force on the jth mechanical mode F_j is written as

$$F_j = (x^{\rm ZPF})^{-1}\sum_{k}^{M}(g_{k,j}a_k^{\dagger} + g_{k,j}^{*}a_k). \tag{C4}$$

Substituting Eq. (B2) into S_j^{FF} and only keeping the quantum noise input $a_k^{\rm in}$, it is derived that

$$S_j^{FF}(\omega) = (x^{\rm ZPF})^{-2}\sum_{k=1}^{M}\frac{|g_{k,j}|^2}{(\omega-\delta_k)^2 + \frac{\kappa_k^2}{4}}. \tag{C5}$$

The quantum cooling limit can be calculated as

$$n_j^{\rm Q} = \frac{S_j^{FF}(-\bar{\omega}_{\rm mec})}{S_j^{FF}(\bar{\omega}_{\rm mec}) - S_j^{FF}(-\bar{\omega}_{\rm mec})}. \tag{C6}$$

Given $\delta_k = \bar{\omega}_{\rm mec}$, $\kappa_k = \kappa$, this expression reduces to

$$n_j^{\rm Q} = \frac{\kappa^2}{16\bar{\omega}_{\rm mec}^2}, \tag{C7}$$

thus the quantum cooling limit does not depend on $\boldsymbol{G}$ under the current approximation, and the result is the same as the

single-mode case. In the resolved-sideband regime investigated in the main text with $\bar{\omega}_{\rm mec} = 20\kappa$, the quantum cooling limit of every mechanical mode $n_j^{\rm Q} < 10^{-3}$, which is negligible compared with the classical cooling limit.

[1] M. Aspelmeyer, T. J. Kippenberg, and F. Marquardt, Cavity optomechanics, Rev. Mod. Phys. **86**, 1391 (2014).

[2] C. F. Ockeloen-Korppi, E. Damskägg, J.-M. Pirkkalainen, M. Asjad, A. A. Clerk, F. Massel, M. J. Woolley, and M. A. Sillanpää, Stabilized entanglement of massive mechanical oscillators, Nature (London) **556**, 478 (2018).

[3] R. Riedinger, A. Wallucks, I. Marinković, C. Löschnauer, M. Aspelmeyer, S. Hong, and S. Gröblacher, Remote quantum entanglement between two micromechanical oscillators, Nature (London) **556**, 473 (2018).

[4] C. F. Ockeloen-Korppi, E. Damskägg, J.-M. Pirkkalainen, A. A. Clerk, M. J. Woolley, and M. A. Sillanpää, Quantum Backaction Evading Measurement of Collective Mechanical Modes, Phys. Rev. Lett. **117**, 140401 (2016).

[5] F. Massel, S. U. Cho, J.-M. Pirkkalainen, P. J. Hakonen, T. T. Heikkilä, and M. A. Sillanpää, Multimode circuit optomechanics near the quantum limit, Nat. Commun. **3**, 987 (2012).

[6] J.-Q. Liao and L. Tian, Macroscopic Quantum Superposition in Cavity Optomechanics, Phys. Rev. Lett. **116**, 163602 (2016).

[7] B. Pepper, R. Ghobadi, E. Jeffrey, C. Simon, and D. Bouwmeester, Optomechanical Superpositions via Nested Interferometry, Phys. Rev. Lett. **109**, 023601 (2012).

[8] J.-Q. Liao, Q.-Q. Wu, and F. Nori, Entangling two macroscopic mechanical mirrors in a two-cavity optomechanical system, Phys. Rev. A **89**, 014302 (2014).

[9] S. Mancini, V. Giovannetti, D. Vitali, and P. Tombesi, Entangling Macroscopic Oscillators Exploiting Radiation Pressure, Phys. Rev. Lett. **88**, 120401 (2002).

[10] L. F. Wei, Y.-x. Liu, C. P. Sun, and F. Nori, Probing Tiny Motions of Nanomechanical Resonators: Classical or Quantum Mechanical?, Phys. Rev. Lett. **97**, 237201 (2006).

[11] M. Poot and H. S. van der Zant, Mechanical systems in the quantum regime, Phys. Rep. **511**, 273 (2012).

[12] T. Liu, F. Pagliano, R. van Veldhoven, V. Pogoretskiy, Y. Jiao, and A. Fiore, Integrated nano-optomechanical displacement sensor with ultrawide optical bandwidth, Nat. Commun. **11**, 2407 (2020).

[13] F. Fogliano, B. Besga, A. Reigue, L. Mercier de Lépinay, P. Heringlake, C. Gouriou, E. Eyraud, W. Wernsdorfer, B. Pigeau, and O. Arcizet, Ultrasensitive nano-optomechanical force sensor operated at dilution temperatures, Nat. Commun. **12**, 4124 (2021).

[14] A. G. Krause, M. Winger, T. D. Blasius, Q. Lin, and O. Painter, A high-resolution microchip optomechanical accelerometer, Nat. Photonics **6**, 768 (2012).

[15] S. Mancini, D. Vitali, and P. Tombesi, Optomechanical Cooling of a Macroscopic Oscillator by Homodyne Feedback, Phys. Rev. Lett. **80**, 688 (1998).

[16] I. Wilson-Rae, N. Nooshi, W. Zwerger, and T. J. Kippenberg, Theory of Ground State Cooling of a Mechanical Oscillator Using Dynamical Backaction, Phys. Rev. Lett. **99**, 093901 (2007).

[17] F. Marquardt, J. P. Chen, A. A. Clerk, and S. M. Girvin, Quantum Theory of Cavity-Assisted Sideband Cooling of Mechanical Motion, Phys. Rev. Lett. **99**, 093902 (2007).

[18] Y.-C. Liu, Y.-F. Xiao, X. Luan, and C. W. Wong, Dynamic Dissipative Cooling of a Mechanical Resonator in Strong Coupling Optomechanics, Phys. Rev. Lett. **110**, 153606 (2013).

[19] Y.-C. Liu, Y.-F. Xiao, X. Luan, Q. Gong, and C. W. Wong, Coupled cavities for motional ground-state cooling and strong optomechanical coupling, Phys. Rev. A **91**, 033818 (2015).

[20] Y.-S. Park and H. Wang, Resolved-sideband and cryogenic cooling of an optomechanical resonator, Nat. Phys. **5**, 489 (2009).

[21] T. Rocheleau, T. Ndukum, C. Macklin, J. B. Hertzberg, A. A. Clerk, and K. C. Schwab, Preparation and detection of a mechanical resonator near the ground state of motion, Nature (London) **463**, 72 (2010).

[22] R. Rivière, S. Deléglise, S. Weis, E. Gavartin, O. Arcizet, A. Schliesser, and T. J. Kippenberg, Optomechanical sideband cooling of a micromechanical oscillator close to the quantum ground state, Phys. Rev. A **83**, 063835 (2011).

[23] J. D. Teufel, T. Donner, D. Li, J. W. Harlow, M. S. Allman, K. Cicak, A. J. Sirois, J. D. Whittaker, K. W. Lehnert, and R. W. Simmonds, Sideband cooling of micromechanical motion to the quantum ground state, Nature (London) **475**, 359 (2011).

[24] J. Chan, T. P. M. Alegre, A. H. Safavi-Naeini, J. T. Hill, A. Krause, S. Gröblacher, M. Aspelmeyer, and O. Painter, Laser cooling of a nanomechanical oscillator into its quantum ground state, Nature (London) **478**, 89 (2011).

[25] E. Verhagen, S. Deléglise, S. Weis, A. Schliesser, and T. J. Kippenberg, Quantum-coherent coupling of a mechanical oscillator to an optical cavity mode, Nature (London) **482**, 63 (2012).

[26] J. Guo, R. Norte, and S. Gröblacher, Feedback Cooling of a Room Temperature Mechanical Oscillator close to its Motional Ground State, Phys. Rev. Lett. **123**, 223602 (2019).

[27] C. Whittle *et al.*, Approaching the motional ground state of a 10-kg object, Science **372**, 1333 (2021).

[28] G. Heinrich, M. Ludwig, J. Qian, B. Kubala, and F. Marquardt, Collective Dynamics in Optomechanical Arrays, Phys. Rev. Lett. **107**, 043603 (2011).

[29] M. Ludwig and F. Marquardt, Quantum Many-Body Dynamics in Optomechanical Arrays, Phys. Rev. Lett. **111**, 073603 (2013).

[30] A. Xuereb, C. Genes, G. Pupillo, M. Paternostro, and A. Dantan, Reconfigurable Long-Range Phonon Dynamics in Optomechanical Arrays, Phys. Rev. Lett. **112**, 133604 (2014).

[31] K. Stannigel, P. Komar, S. J. M. Habraken, S. D. Bennett, M. D. Lukin, P. Zoller, and P. Rabl, Optomechanical Quantum Information Processing with Photons and Phonons, Phys. Rev. Lett. **109**, 013603 (2012).

[32] V. Fiore, Y. Yang, M. C. Kuzyk, R. Barbour, L. Tian, and H. Wang, Storing Optical Information as a Mechanical Excitation in a Silica Optomechanical Resonator, Phys. Rev. Lett. **107**, 133601 (2011).

[33] H. Okamoto, A. Gourgout, C.-Y. Chang, K. Onomitsu, I. Mahboob, E. Y. Chang, and H. Yamaguchi, Coherent phonon manipulation in coupled mechanical resonators, Nat. Phys. **9**, 480 (2013).

[34] Y.-D. Wang and A. A. Clerk, Using Interference for High Fidelity Quantum State Transfer in Optomechanics, Phys. Rev. Lett. **108**, 153603 (2012).

[35] P. A. Truitt, J. B. Hertzberg, C. C. Huang, K. L. Ekinci, and K. C. Schwab, Efficient and sensitive capacitive readout of nanomechanical resonator arrays, Nano Lett. **7**, 120 (2007).

[36] I. Bargatin, E. B. Myers, J. S. Aldridge, C. Marcoux, P. Brianceau, L. Duraffourg, E. Colinet, S. Hentz, P. Andreucci, and M. L. Roukes, Large-scale integration of nanoelectromechanical systems for gas sensing applications, Nano Lett. **12**, 1269 (2012).

[37] P. Rabl, S. J. Kolkowitz, F. H. L. Koppens, J. G. E. Harris, P. Zoller, and M. D. Lukin, A quantum spin transducer based on nanoelectromechanical resonator arrays, Nat. Phys. **6**, 602 (2010).

[38] P. Huang, P. Wang, J. Zhou, Z. Wang, C. Ju, Z. Wang, Y. Shen, C. Duan, and J. Du, Demonstration of Motion Transduction Based on Parametrically Coupled Mechanical Resonators, Phys. Rev. Lett. **110**, 227202 (2013).

[39] P. Huang, L. Zhang, J. Zhou, T. Tian, P. Yin, C. Duan, and J. Du, Nonreciprocal Radio Frequency Transduction in a Parametric Mechanical Artificial Lattice, Phys. Rev. Lett. **117**, 017701 (2016).

[40] C. Genes, D. Vitali, and P. Tombesi, Simultaneous cooling and entanglement of mechanical modes of a micromirror in an optical cavity, New J. Phys. **10**, 095009 (2008).

[41] C. Sommer and C. Genes, Partial Optomechanical Refrigeration via Multimode Cold-Damping Feedback, Phys. Rev. Lett. **123**, 203605 (2019).

[42] A. B. Shkarin, N. E. Flowers-Jacobs, S. W. Hoch, A. D. Kashkanova, C. Deutsch, J. Reichel, and J. G. E. Harris, Optically Mediated Hybridization between Two Mechanical Modes, Phys. Rev. Lett. **112**, 013602 (2014).

[43] C. F. Ockeloen-Korppi, M. F. Gely, E. Damskägg, M. Jenkins, G. A. Steele, and M. A. Sillanpää, Sideband cooling of nearly degenerate micromechanical oscillators in a multimode optomechanical system, Phys. Rev. A **99**, 023826 (2019).

[44] D.-G. Lai, F. Zou, B.-P. Hou, Y.-F. Xiao, and J.-Q. Liao, Simultaneous cooling of coupled mechanical resonators in cavity optomechanics, Phys. Rev. A **98**, 023860 (2018).

[45] X. Y. Zhang, Y. H. Zhou, Y. Q. Guo, and X. X. Yi, Simultaneous cooling of two mechanical oscillators in dissipatively coupled optomechanical systems, Phys. Rev. A **100**, 023807 (2019).

[46] D.-G. Lai, J.-F. Huang, X.-L. Yin, B.-P. Hou, W. Li, D. Vitali, F. Nori, and J.-Q. Liao, Nonreciprocal ground-state cooling of multiple mechanical resonators, Phys. Rev. A **102**, 011502(R) (2020).

[47] S. J. M. Habraken, K. Stannigel, M. D. Lukin, P. Zoller, and P. Rabl, Continuous mode cooling and phonon routers for phononic quantum networks, New J. Phys. **14**, 115004 (2012).

[48] S. Kim, X. Xu, J. M. Taylor, and G. Bahl, Dynamically induced robust phonon transport and chiral cooling in an optomechanical system, Nat. Commun. **8**, 205 (2017).

[49] H. Xu, L. Jiang, A. A. Clerk, and J. G. Harris, Nonreciprocal control and cooling of phonon modes in an optomechanical system, Nature (London) **568**, 65 (2019).

[50] K.-J. Boller, A. Imamoğlu, and S. E. Harris, Observation of Electromagnetically Induced Transparency, Phys. Rev. Lett. **66**, 2593 (1991).

[51] T. P. Purdy, R. W. Peterson, P.-L. Yu, and C. A. Regal, Cavity optomechanics with Si_3N_4 membranes at cryogenic temperatures, New J. Phys. **14**, 115021 (2012).

[52] A. M. Jayich, J. C. Sankey, B. M. Zwickl, C. Yang, J. D. Thompson, S. M. Girvin, A. A. Clerk, F. Marquardt, and J. G. E. Harris, Dispersive optomechanics: a membrane inside a cavity, New J. Phys. **10**, 095008 (2008).

[53] P.-L. Yu, T. P. Purdy, and C. A. Regal, Control of Material Damping in High-q Membrane Microresonators, Phys. Rev. Lett. **108**, 083603 (2012).

[54] R. A. Norte, J. P. Moura, and S. Gröblacher, Mechanical Resonators for Quantum Optomechanics Experiments at Room Temperature, Phys. Rev. Lett. **116**, 147202 (2016).

[55] C. K. Law, Interaction between a moving mirror and radiation pressure: A Hamiltonian formulation, Phys. Rev. A **51**, 2537 (1995).

[56] L. Praxmeyer and K. G. Zloshchastiev, Master equation approach for non-Hermitian quadratic hamiltonians: Original and phase space formulations, J. Phys.: Conf. Ser. **1194**, 012090 (2019).